

Regulation of blood cell transdifferentiation by oxygen sensing neurons in *Drosophila*

Sean Corcoran², Anjeli Mase², Yousuf Hashmi², Debra Ouyang², Jordan Augsburg², Thea Jacobs²,
Katelyn Kukar², Katja Brückner^{1, 2, 3, 4}

¹Eli and Edythe Broad Center of Regeneration Medicine and Stem Cell Research

²Department of Cell and Tissue Biology

³Cardiovascular Research Institute, University of California San Francisco, San Francisco, CA

⁴Corresponding Author:

35 Medical Center Way

San Francisco, CA 94143-066

e-mail: katja.brueckner@ucsf.edu

Highlights

- Functional lineage tracing confirms in vivo transdifferentiation in a *Drosophila* model of hematopoiesis
- Blood cell transdifferentiation is promoted by active sensory neurons of the caudal sensory cones of the *Drosophila* larva
- Sensory cone neurons detect oxygen through atypical guanylyl cyclases and promote blood cell transdifferentiation

Keywords

Drosophila, transdifferentiation, hematopoiesis, microenvironment, hemocyte, macrophage, plasmacyte, crystal cell, sensory neurons, sensory cones, atypical guanylyl cyclases, oxygen sensing, hypoxia

Summary

Transdifferentiation of functionally specialized cell types, which omits the need for stem or progenitor cells, is known across the animal kingdom. However, in the blood cell system it remains largely unclear how transdifferentiation is regulated in vivo. Here we reveal the environmental control of blood cell transdifferentiation in a *Drosophila melanogaster* model. Functional lineage tracing provides new in vivo evidence for direct transdifferentiation from macrophage-like plasmatocytes to crystal cells that execute melanization. Interestingly, this transdifferentiation is promoted by neuronal activity of a specific subset of sensory neurons, in the sensory cones at the caudal end of the larva. Evidence for this stems from specific neuron ablation, and transient silencing or activation of these neurons by *Kir2.1* or *TrpA1*, respectively. Crystal cells develop from plasmatocytes in clusters surrounding the sensory cones. Strikingly, environmental conditions trigger this process: oxygen sensing, through atypical guanylyl cyclases (Gyc88E, Gyc89Da, Gyc89Db) that are specifically expressed in sensory cone neurons, drives plasmatocyte-to-crystal cell transdifferentiation, as hypoxia or gyc silencing cause crystal cell reduction and loss of transdifferentiation. Our findings reveal an unexpected functional and molecular link of environment-monitoring sensory neurons governing blood cell transdifferentiation in vivo, suggesting similar principles in vertebrate systems where environmental sensors and blood cell populations coincide.

Results and Discussion

A Drosophila model of blood cell transdifferentiation

Transdifferentiation is known in many species including vertebrates (Cieslar-Pobuda et al., 2017; Reid and Tursun, 2018), but in the blood cell system transdifferentiation has for the most part only been studied in vitro and by experimental manipulations. For example, C/EBP (CCAAT/enhancer-binding protein) transcription factors drive transdifferentiation of vertebrate B cells into macrophages (Xie et al., 2004) (Di Tullio et al., 2011), force B lymphoma and leukemia cell lines to transdifferentiate into macrophages (Rapino et al., 2013), and facilitate B cell transdifferentiation to Granulocyte-Macrophage Precursors (Cirovic et al., 2017). Similarly, manipulation of key transcription factors such as FLI1 and ERG result in transdifferentiation of erythroblasts to megakaryocytes (Siripin et al., 2015), and deletion of the BAF Chromatin Remodeling Complex Subunit Bcl11b triggers T cell transition to NK cells (Li et al., 2010). Transdifferentiation of lymphoid and myeloid cells has been modeled mathematically (Collombet et al., 2017). However, in vivo, the underlying cellular and molecular mechanisms of blood cell transdifferentiation during development and homeostasis and the role of the environment remain elusive.

To investigate principles of in vivo transdifferentiation in the hematopoietic system, we turned to a model in the fruit fly, *Drosophila melanogaster*. *Drosophila* offers versatile genetics and proven parallels to vertebrate hematopoiesis. Similar to the two major lineages that produce myeloid blood cells in vertebrates (Davies et al., 2013; Perdiguero and Geissmann, 2016; Sieweke and Allen, 2013), *Drosophila* gives rise to two myeloid lineages of blood cells, or hemocytes (Gold and Brückner, 2014, 2015; Holz et al., 2003), (1) the embryonic lineage of hemocytes that proliferate as differentiated cells in hematopoietic pockets of the larval body wall, and resemble vertebrate tissue macrophages, and (2) the progenitor-based lymph gland lineage (Banerjee et al., 2019). Both *Drosophila* blood cell lineages produce at least three differentiated blood cell types: macrophage-like plasmatocytes, crystal cells that mediate melanization, and lamellocytes, large immune cells specialized for encapsulation (Banerjee et al., 2019; Gold and Brückner, 2014, 2015). During larval stages, embryonic-lineage plasmatocytes show signs of fate changes to other blood cell types: Transdifferentiation to lamellocytes occurs in response to immune challenges (Markus et al., 2009), and crystal cells derive from plasmatocytes through transdifferentiation, even under steady state conditions (Leitao and Sucena, 2015). While it was suggested that Notch signaling between plasmatocytes contributes to the formation of crystal cells (Leitao and Sucena, 2015), there is still

little understanding of the anatomical requirements and molecular signaling pathways that regulate plasmatocyte-to-crystal cell transdifferentiation in vivo. Hematopoietic sites of the *Drosophila* larva contain sensory neuron clusters of the peripheral nervous system (PNS) that serve as microenvironments for plasmatocyte survival, proliferation and localization (Gold and Brückner, 2014, 2015; Makhijani et al., 2017; Makhijani et al., 2011; Makhijani and Brückner, 2012). Considering this, we investigated the role of these specialized hematopoietic pockets in hemocyte transdifferentiation.

Phagocytic plasmatocytes give rise to differentiated crystal cells

First, we examined the formation of crystal cells and their anatomical locations during larval development. We used a traditional way of labeling and quantifying crystal cells based on their expression of prophenoloxidasases (Corcoran and Brückner, 2020; Rizki and Rizki, 1959), enzymes responsible for melanization, the main immune function of crystal cells (Bidla et al., 2009; Dudzic et al., 2015; Lu et al., 2014). Experimental induction of melanization blackens crystal cells (Corcoran and Brückner, 2020; Rizki and Rizki, 1959) and marks similar cell populations as the crystal cell driver/ reporter *lozenge-GAL4* (*lz-GAL4*; *UAS-GFP*) (SupplFig. 1 A, B).

During larval development, crystal cell numbers increase slowly over the first and second larval instar stages, but expand more rapidly during the third instar stage (Fig. 1 A). This exponential increase overall follows the increase in plasmatocytes during larval development (Fig 1 B) (Makhijani et al., 2011; Petraki et al., 2015). To visualize crystal cells and plasmatocytes, we coexpressed two fluorescent protein reporters (for crystal cells *BcF2-GFP* (Tokusumi et al., 2009), and for plasmatocytes *HmlΔ-DsRed* (Makhijani et al., 2011)). Crystal cells are strongly enriched in a cluster in the terminal segment of the *Drosophila* larva, a region where plasmatocytes are also known to accumulate (Fig. 1 C-C'', D-D') (Makhijani et al., 2011). Crystal cells are occasionally also found in other hematopoietic pockets, and in dorsal vessel-associated clusters where floating hemocytes accumulate (Cevik et al., 2019; Petraki et al., 2015).

Since previous studies suggested plasmatocyte-to-crystal cell transdifferentiation based on live imaging (Leitao and Sucena, 2015), we chose to confirm the current model by an independent lineage tracing approach. Asking whether crystal cells derive from undifferentiated progenitors or differentiated, phagocytically active plasmatocytes, we established a cell tracing approach based on the unique ability of differentiated plasmatocytes to phagocytically uptake fluorescently labeled beads (Fig. 1 E-E'''). We injected *Drosophila* larvae expressing fluorescent reporters for

plasmatocytes and crystal cells with blue fluorescent latex beads. Injected larvae were incubated in a time course, followed by the release of hemocytes and quantification of the relative fractions of phagocytosis-labeled plasmatocytes and -crystal cells (Fig. 1 F, G). The fraction of blue bead positive plasmatocytes quickly reached saturation (~50% at 1h, ~90% at 4h and 22h). In contrast, crystal cells were labeled by blue beads with a significant time delay (<10% at 1h, ~ 50% at 4h, ~70% at 22h) (Fig. 1 G). Together with previous reports that suggested crystal cells are not capable of phagocytosis themselves (Lanot et al., 2001; Leitao and Sucena, 2015) this supports a model of plasmatocyte-to-crystal cell transdifferentiation, in which crystal cells derive from phagocytically active plasmatocytes, rather than from undifferentiated, phagocytosis-incompetent progenitors.

Sensory neuron activity promotes crystal cell transdifferentiation

Next, we investigated the anatomical locations of crystal cells and plasmatocytes relative to sensory neurons, using fluorescent reporters and live imaging; sensory neurons were labeled by a specific driver (*21-7-GAL4*, *UAS-CD8-GFP* (Song et al., 2007)) (Fig. 2 A). We found that both plasmatocytes and crystal cells colocalize with sensory neurons, with one important difference: plasmatocytes are found in all hematopoietic pockets (Fig. 2 A), while crystal cells are mainly localized in the terminal hematopoietic pocket of the larva (Fig. 2 B).

Given this colocalization with sensory neurons, we asked whether sensory neuron activity has an effect on crystal cell generation. To mimic activation of sensory neurons, we exposed larvae to the acetylcholine receptor agonist carbamoycholine (carbachol). Carbachol exposure over 4 hours resulted in a moderate increase of crystal cell numbers (Fig. 2 C). More specifically and complementary to this, we silenced sensory neurons by transient expression of *Kir2.1*, an inward rectifying K⁺ channel that causes neuron hyperpolarization (Baines et al., 2001). Interestingly, *Kir2.1* expression over 22 hours caused a dramatic drop in crystal cell numbers (Fig. 2 D). There was no significant effect of neuronal silencing on total hemocyte numbers under comparable conditions (SupplFig. 2 and (Makhijani et al., 2017)). To address whether sensory neuron silencing by *Kir2.1* affects plasmatocyte to crystal cell transdifferentiation, we performed phagocytosis lineage tracing. Indeed, transient neuronal silencing affects the fraction of crystal cells derived from blue bead labeled plasmatocytes, while the ability of plasmatocytes to phagocytose remains the same (Fig. 2 E, F). Taken together, our findings suggest that sensory neuron activity promotes transdifferentiation of plasmatocytes to crystal cells.

Crystal cells colocalize with, and require, sensory neurons of the sensory cones

To gain more insight, we focused on the caudal cluster of crystal cells. Closer inspection of combined fluorescent reporters for crystal cells and sensory neurons showed that crystal cells colocalize particularly well with sensory organs of the sensory cones (Fig. 3 A-A'' and C-D'), protruding structures that are grouped around the posterior spiracles, the terminal tubes of the tracheal system (Hayashi and Kondo, 2018; Kuhn et al., 1992). Plasmotocytes also accumulate in a large cluster around the sensory cones (Fig. 3 B-B''). Interestingly, the pattern and abundance of crystal cells in the 3rd instar larva resemble plasmotocytes in the 2nd instar larva (Fig. 3 B-B'' and D-D'). We therefore hypothesized that many plasmotocytes of the 2nd instar larva may transdifferentiate to crystal cells, as is apparent in the 3rd instar.

Given the intriguing colocalization of crystal cells and sensory neurons and the dependence of blood cell transdifferentiation on neuronal activity, we investigated the specific requirement of sensory cone neurons for crystal cell production. A group of genes specifically expressed in sensory cone neurons are atypical guanylyl cyclases, *Gyc88E*, *Gyc89Da*, and *Gyc89Db* (Vermehren-Schmaedick et al., 2010). Using the driver *Gyc89Db-GAL4* (Vermehren-Schmaedick et al., 2010) (Fig. 3 E, F), we ablated sensory cone neurons by expressing the proapoptotic gene *head involution defect* (*Hid*) in its non-repressible version (*Hid^{ala5}*) (Bergmann et al., 2002). Ablation of sensory cone neurons did not affect larval viability, but it strongly reduced crystal cell numbers (Fig. 3 G). Conversely, ectopic activation of sensory cone neurons by specific expression and transient induction of the heat-induced cation channel TrpA1 (Hamada et al., 2008) caused a significant increase in crystal cells (Fig. 3 H). Taken together, we conclude that crystal cells and their precursor plasmotocytes are strongly enriched at the sensory cones of the larva. Sensory cone neurons, and their activity, are required for crystal cells.

Oxygen sensing through atypical guanylyl cyclases drives plasmotocyte-to-crystal cell transdifferentiation

The atypical guanylylcyclases *Gyc88E*, *Gyc89Da*, and *Gyc89Db* are described as cytoplasmic oxygen sensors, which form heterodimers of *Gyc88E* and either *Gyc89Da* or *Gyc89Db*, and *Gyc88E* homodimers (Morton, 2004; Morton et al., 2005; Vermehren et al., 2006). Activated Gyc complexes generate the second messenger cyclic GMP (cGMP) which in turn activates neurons (Morton, 2004; Morton et al., 2008). Since we found that sensory cone neurons expressing these genes are required for crystal cell formation, we decided to test Gyc function itself in relation to crystal cell transdifferentiation. When the major subunit, *Gyc88E*, was silenced in the sensory cone neurons,

crystal cell numbers were reduced (Fig. 4 A). Phagocytosis lineage tracing confirmed that Gyc function is required for transdifferentiation of plasmatocytes to crystal cells, as the fraction of crystal cells carrying blue beads was significantly reduced in *Gyc88E* RNAi knockdowns, while phagocytosis by plasmatocytes remained the same (Fig. 4 B). Given the role of GyCs as oxygen sensors, we next investigated the effect of varying atmospheric oxygen concentrations on crystal cell formation. Assessing crystal cell numbers per larva as readout, we exposed larvae to 5% or 8% oxygen for 6 hours. Compared to normoxia (~21% oxygen), both levels of hypoxia caused some reduction in crystal cells, while total hemocyte numbers stayed constant (SupplFig. 3 A, B, Fig. 4 C). More robust results were obtained under 5% oxygen, which we decided to pursue further (Fig. 4 C). To determine whether hypoxia affects blood cell transdifferentiation, we performed phagocytosis lineage tracing for 6 hours under hypoxic conditions (5% O₂) and normoxia. Interestingly, hypoxia phenocopies silencing of gyc function in sensory cone neurons, resulting in a significant reduction of blue beads in crystal cells, while phagocytosis levels of plasmatocytes remain unaffected (Fig. 4 D). We therefore conclude that oxygen sensing through atypical guanylyl cyclases (GyCs) in the sensory cone neurons that is linked to neuron activation drives plasmatocyte-to-crystal cell transdifferentiation (Fig. 4 E). This model supports the kinetics of crystal cells following plasmatocyte expansion, based on the transition of plasmatocytes to crystal cells in particular in the proximity of sensory cone neurons (SupplFig. 4 A).

Conclusions

Our work has identified an unexpected mechanistic link between oxygen sensing and blood cell transdifferentiation, which is facilitated through a particular set of sensory neurons and intracellular Gyc oxygen sensors. This new paradigm inspires the search for similar principles of neuronally controlled blood cell transdifferentiation that responds to environmental conditions in other species including humans.

Transdifferentiation results in the conversion of one differentiated cell type to another. In some systems, new differentiated cell types arise after de-differentiation to a transient pluripotent intermediate (Pesaresi et al., 2019; Reid and Tursun, 2018). Our work supports a model of direct transdifferentiation based on fluorescent reporters and phagocytosis lineage tracing, although these methods cannot rule out the possibility of brief periods of de-differentiation. However, independent approaches also support a model of continuous blood cell transdifferentiation from plasmatocytes to crystal cells through progressive states, based on single cell RNAseq pseudotime lineage analysis

(Tattikota et al., 2019). Transdifferentiation may be the fastest and most efficient way for animals to shape the composition of their blood cell pool according to environmental conditions such as oxygen levels and potentially other inputs.

Gyc intracellular oxygen sensors mediate oxygen detection in sensory neurons (Vermehren et al., 2006), similar to other oxygen sensing mechanisms known in vertebrate neurons and other sensory cells (Caravagna and Seaborn, 2016; Pokorski et al., 2016). In contrast, HIF (hypoxia inducible factor) transcription factors regulate target genes in response to low oxygen conditions in a variety of cell types (Gorr et al., 2006; Majmundar et al., 2010). Hypoxia, through HIF, regulates mammalian hematopoiesis, lymphopoiesis and erythropoiesis (Chabi et al., 2019; Haase, 2013; Imanirad and Dzierzak, 2013). The *Drosophila* HIF1 α *sima* (*similar*) plays a role in crystal cell formation in the *Drosophila* lymph gland (Mukherjee et al., 2011), however this effect is independent of HIF1 β (*tango* in *Drosophila*) and hypoxia target genes. Instead, Sima activates Notch signaling through a noncanonical mechanism (Mukherjee et al., 2011). Notch signaling has been associated with crystal cell production in *Drosophila* throughout development, in the embryo (Lebestky et al., 2000), in the lymph gland (Duvic et al., 2002; Krzemien et al., 2007; Lebestky et al., 2003) and in embryonic-lineage hemocytes in the larva (Duvic et al., 2002; Leitao and Sucena, 2015). In the latter, plasmacyte-to-crystal cell transdifferentiation was suggested to be controlled by Notch (N) signaling through plasmacyte-plasmacyte contacts in resident clusters (Leitao and Sucena, 2015). It remains to be determined whether oxygen sensing neurons and/or the signal receiving plasmacytes are connected to Notch signaling or an independent pathway that governs the fate switch of plasmacytes to crystal cells.

Linking oxygen sensing to crystal cell formation via Gycs could have several advantages. Oxygen sensing by neurons is more sensitive and immediate, responding directly to environmental conditions. Sensory cone neurons are at all times in contact with the surrounding atmosphere. *Drosophila* larvae display social burying behaviors during feeding, exposing their caudal ends with the sensory cones and allowing air intake to the tracheal system through the neighboring posterior spiracles (Hayashi and Kondo, 2018; Wu et al., 2003) (SupplFig. 4 B); mature 3rd instar larvae then exit the food source to eventually pupariate (Wu et al., 2003) (SupplFig. 4 B). With their exposed nature, these sensory neurons may also integrate other inputs from the environment (Stewart et al., 2015; Vermehren-Schmaedick et al., 2011; Xiang et al., 2010) when communicating to their targets.

Activation of the sensory cone neurons coordinates blood cell transdifferentiation with other responses to hypoxia: Oxygen sensing by GyCs in the sensory cone neurons have been linked to a behavioral escape response to hypoxic conditions (Morton, 2011; Vermehren-Schmaedick et al., 2010). GyCs generate cGMP, which activates cyclic nucleotide gated channels (CNG) (Morton et al., 2008; Vermehren-Schmaedick et al., 2010). CNG channels mediate influx of calcium ions, resulting in consecutive activation of calmodulin/CaMK signaling and sensory transduction (Kaupp and Seifert, 2002; Pifferi et al., 2006).

Neuronal regulation of the hematopoietic system and other organs is an important paradigm in biology, which has started to come to light in a variety of species (Kumar and Bröckner, 2012). In *Drosophila*, neuronal regulation of hematopoiesis is well established. Embryonic-lineage plasmatocytes depend on sensory neurons for their survival, proliferation and localization (Gold and Brückner, 2014, 2015; Makhijani et al., 2017; Makhijani et al., 2011; Makhijani and Brückner, 2012). Specifically, Activin- β , a TGF- β family ligand, is a key signal produced by active sensory neurons that promotes plasmatocyte proliferation and adhesion (Makhijani et al., 2017). Identification of the signal/s mediating communication from active sensory cone neurons to plasmatocytes that trigger transdifferentiation will be a matter of future study. We postulate signaling by a secreted factor, which could potentially, albeit at reduced efficiency, also act at a distance, promoting smaller numbers of crystal cells develop from plasmatocytes in the dorsal vessel associated hemocyte clusters (Leitao and Sucena, 2015) and segmental hematopoietic pockets. In this context, it is interesting to note that, in long term memory formation, Activin expression is induced downstream of calmodulin/CaMK/CREB signaling in both *Drosophila* and vertebrates (Inokuchi et al., 1996; Miyashita et al., 2012), suggesting potential parallels in the role this signaling cassette could play in neuron-induced blood cell transdifferentiation.

In vertebrates, the autonomic nervous system regulates aspects of bone marrow hematopoiesis and inflammatory responses (Hanoun et al., 2015; Pavlov and Tracey, 2012), but links of hematopoiesis with sensory neurons or other sensing systems have remained largely unknown. Oxygen exposure and sensing could be an important regulatory factor in more recently identified hematopoietic sites such as the vertebrate lung, which harbors limited blood cell progenitors and megakaryocytes that are active in platelet production (Lefrancais et al., 2017; Martin et al., 1983). The lung, like many other organs, also harbors tissue macrophages that proliferate in local microenvironments and bear evolutionary parallels with *Drosophila* embryonic-lineage plasmatocytes (Gold and Brückner, 2014, 2015; Perdiguero and Geissmann, 2016). Interestingly, in the vertebrate lung, neuroendocrine cells,

distributed as solitary cells and as innervated clusters, have roles as oxygen sensing cells early in life, and later provide a microenvironment for airway epithelial cells (Caravagna and Seaborn, 2016; Cutz et al., 2007). The lung and airways are also rich in vagal afferent nerves that sense various chemical and mechanical cues (Chang et al., 2015; Mazzone and Udem, 2016). In vertebrates, it will therefore be interesting to investigate the role of sensory neurons and other sensors in the regulation of hematopoiesis, transdifferentiation, and immune cell fate and function.

Materials and Methods

Drosophila Strains

Drosophila drivers, reporters and related lines used were *HmlΔ-GAL4*, *UAS-GFP* (Sinenko and Mathey-Prevot, 2004); combination driver *HmlΔGAL4*, *UAS-GFP*; *He-GAL4* ((Yang et al., 2015) gift from Dan Hultmark), *Iz-GAL4*; *UAS-GFP* (J. Pollock, Bloomington), *21-7-GAL4* (Makhijani et al., 2011; Song et al., 2007) *Gyc89Db-GAL4* (Morton et al., 2008); *BcF6-GFP* (Tokusumi et al., 2009), *BcF6-mCherry* (Tokusumi et al., 2009), *BcF2-GFP* (Tokusumi et al., 2009); *HmlΔ-DsRed* (Makhijani et al., 2011); and *tubGAL80ts* (McGuire et al., 2003). UAS lines used were *UAS-GFP* (Song et al., 2007); *UAS-CD8-GFP* (Song et al., 2007); *UAS-Kir2.1* (Baines et al., 2001) (Bloomington); *UAS-TrpA1* (Bloomington); *UAS-Hid ala5* (Bergmann et al., 2002); *UAS-Gyc88E RNAi* (Bloomington). Control lines used were *w1118* (Bloomington) or *yw* (Bloomington). Unless otherwise stated, fly crosses were set and maintained at 25° Celsius. Crosses with the driver *Gyc89Db-GAL4* were performed at 29°C to increase expression.

Hemocyte Quantification

Total hemocyte quantification was performed essentially as described in (Corcoran and Brückner, 2020; Petraki et al., 2015). All fluorescently-marked hemocytes of single larvae were released into wells marked by a hydrophobic PAP pen (Beckman Coulter) on glass slides filled with 20-30 µL PBS. Cells were allowed to settle for 15-20 min, and were imaged by fluorescence tile scan microscopy on a Leica DMI4000B microscope with Leica DFC350FX camera and 20x objective. Cell numbers in images were analyzed by particle quantification using Fiji/ImageJ (Corcoran and Brückner, 2020; Petraki et al., 2015; Schindelin et al., 2012).

Crystal cell quantification was performed using fluorescent protein reporters or melanization. To quantify crystal cells in live animals, larvae were placed on a slide in a small drop of 10-15 µl PBS

with a coverslip on top. Fluorescent crystal cells in each segment were manually counted, rolling the larva by gently moving the coverslip. For phagocytosis lineage tracing, fluorescent crystal cells were quantified *ex vivo* (see below). To quantify crystal cells based on their ability to melanize (due to their hallmark expression of functional Prophenoloxidase 1 and 2) larvae of desired sizes/ages were placed in 250 μ l of PBS in Eppendorf tubes and heated at 65° Celsius for 22 minutes in a heat block. Heating induces crystal cell melanization visible as black cells, allowing easy *in situ* visualization through the cuticle and manual counting (Corcoran and Brückner, 2020; Rizki and Rizki, 1959).

Unless otherwise noted, larvae were grown at 25°C and analyzed at various developmental times after egg laying (AEL) corresponding to the following size ranges: 1st instar: ~0.5-1.4mm (22-46h AEL); 2nd instar: ~1.5-2.6mm (47-77h AEL); 3rd instar: ~2.7- >3.5mm (from 78h AEL). For the crosses used, no developmental delays were observed; therefore selection of specified larval size ranges from 24h embryo collections was used in lieu of more tightly timed embryo collections.

Manipulation of Neuronal Activity

To mimic sensory neuron stimulation, larvae were exposed to 10mg/ml carbamylcholine (carbachol, Sigma Aldrich) in fly food for 4 hours allowing direct cuticle contact with carbachol (Makhijani et al., 2017).

To activate specific neuron populations, the heat-inducible cation channel TrpA1 was ectopically expressed and transiently heat induced to mimic neuron activation (Hamada et al., 2008). Sopecifically, *TrpA1* crosses were set at RT and shifted to 29°C for 4h. Larvae were analyzed within 30 minutes following this period.

Sensory neuron silencing was achieved by transiently expressing a transgenic of the inward rectifying potassium channel Kir2.1 (Baines et al., 2001), under control of a sensory neuron specific GAL4 driver and a temperature-sensitive GAL4 inhibitor GAL80ts (McGuire et al., 2003); genotypes for neuronal silencing experiments were *21-7-GAL4, UAS-GFP, Hml Δ DsRed/UAS-Kir2.1; tubGAL80ts/+* with controls *21-7-GAL4, UAS-GFP, Hml Δ DsRed/+; tubGAL80ts/+*. F1 from crosses were raised at 18° Celsius. To temporarily silence sensory neurons, larvae were shifted from 18° to 29° Celsius for 22 hours to destabilize GAL80ts, allowing for expression of Kir2.1, which hyperpolarizes sensory neuron preventing firing. Larvae were analyzed within 1 hour post-silencing.

Phagocytosis Lineage Tracing

For lineage tracing of crystal cells that derive from actively phagocytic plasmatocytes, larvae with genotype *HmlΔGAL4, UAS-GFP; BcF6-mCherry* were injected with 69 nl of blue fluorescent FluoSphere Carboxylate-modified 0.2 um beads (Invitrogen) diluted 1:100 in PBS using a Nanoject injector (Drummond Scientific). After injection, larvae were placed on food with yeast for 4 hours. Hemocytes of individual larvae were then released into a well marked on a glass slide by PAP pen and filled with 20-30 μl PBS; hemocytes were allowed to settle for 15-20 minutes in a wet chamber (Corcoran and Brückner, 2020; Petraki et al., 2015). Cells were imaged with a Leica DMI4000 microscope with tilescan function. Cell quantification was conducted manually from a representative central field of each image (containing ~150-300 plasmatocytes). For genotypes that give rise to substantially reduced numbers of crystal cells, crystal cells of the whole tilescan area were analyzed. Transdifferentiation was quantified by comparing ratios of crystal cells positive for blue particles/total crystal cells (mCherry positive) for various experimental and control conditions. The same quantification for plasmatocytes (GFP positive) with blue beads relative to all plasmatocytes was conducted as an internal control for injection efficiency and phagocytic fitness.

Hypoxia experiments

Hypoxia experiments were conducted using a hypoxic chamber (Biospherix, Inc., Laconia, NY). Oxygen concentrations were set as indicated, supplementing reduced O₂ with N₂. Incubations were performed at room temperature (RT) for 6h. Crystal cell melanization assays were conducted with larvae of the genotype *w¹¹¹⁸*, and phagocytic lineage tracing and total hemocyte experiments used *HmlΔ-GAL4, UAS-GFP; BcF6-mCherry* larvae. For all experiments, 15-25 larvae of the desired age/size and genotype were placed on inactivated yeast paste in cell strainer snap cap tubes, allowing for rapid gas exchange (Corning #352235). Six cell strainer tubes were held by a fitted rack that was inserted into a large cylindrical polystyrene *Drosophila* population cage with steel mesh on one side (custom construction). During transport from the hypoxic chamber to the bench, population cages were sealed in a plastic bag to maintain hypoxic conditions up to the point when larvae were analyzed. Control samples were placed in an identical setup but left at normoxic conditions at comparable temperature (RT) and time (6h). Following hypoxia/normoxia conditions, assays were conducted as described in the respective paragraphs.

Microscopy

Released hemocytes were imaged on a Leica DMI4000B microscope as described above. Live imaging of larvae was done as described previously, immobilizing larvae on an ice-cooled metal block (Makhijani et al. *Development* 2011). Imaging was performed using a Leica M205FA fluorescent stereoscope with DFC300FX color digital camera and Leica LAS Montage module, combining z-stacks into single in-focus images.

Statistical Analysis

For all experiments numbers of larvae per genotype and condition are indicated in the Figure Legends. For each genotype and condition the mean and standard deviation were determined and significance was tested by 2-way ANOVA (Prism). For hemocyte counts over the course of larval development, regression analysis was performed (Excel). For phagocytosis lineage tracing, the mean and standard deviation of percentages of blue bead positive cells were determined and assessed by 2-way ANOVA (Prism). P-value cutoffs for significance were as follows: * = $p < 0.05$, ** = $p < 0.01$, and *** = $p < 0.001$. Pools of both male and female larvae were analyzed.

Authors' contributions

KB conceived and supervised the study. SC, AM and KB planned the experiments. SC, AM, JA, YH, DO, TJ, KK carried out the experiments. SC, AM, JA, YH, DO, TJ, KK and KB analyzed the data. KB wrote the manuscript with input from all authors.

Competing interests

The authors have no competing interests.

Funding

This work was supported by grants from the American Cancer Society RSG DDC-122595, American Heart Association 13BGIA13730001, National Science Foundation 1326268, and National Institutes of Health 1R01GM112083, 1R56HL118726 and 1R01GM131094 (to KB).

Acknowledgements

We thank D. Morton, R. Schulz, U. Banerjee, A. Bergmann, C. Evans, D. Hultmark, Y.N. Jan, L. Kockel, the Bloomington Stock Center, and TRiP for fly stocks. We are grateful to Khalida Sabeur and Manideep Chavali for help to access and use hypoxia chamber equipment. Thanks to Ava Brückner-Kockel for advice on regression analysis. We thank members of the Brückner lab for discussion and feedback on the manuscript.

References

- Baines, R.A., Uhler, J.P., Thompson, A., Sweeney, S.T., and Bate, M. (2001). Altered electrical properties in *Drosophila* neurons developing without synaptic transmission. *J Neurosci* 21, 1523-1531.
- Banerjee, U., Girard, J.R., Goins, L.M., and Spratford, C.M. (2019). *Drosophila* as a Genetic Model for Hematopoiesis. *Genetics* 211, 367-417.
- Bergmann, A., Tugentman, M., Shilo, B.Z., and Steller, H. (2002). Regulation of cell number by MAPK-dependent control of apoptosis: a mechanism for trophic survival signaling. *Dev Cell* 2, 159-170.
- Bidla, G., Hauling, T., Dushay, M.S., and Theopold, U. (2009). Activation of insect phenoloxidase after injury: endogenous versus foreign elicitors. *J Innate Immun* 1, 301-308.
- Caravagna, C., and Seaborn, T. (2016). Oxygen Sensing in Early Life. *Lung* 194, 715-722.
- Cevik, D., Acker, M., Michalski, C., and Jacobs, J.R. (2019). Pericardin, a *Drosophila* collagen, facilitates accumulation of hemocytes at the heart. *Dev Biol* 454, 52-65.
- Chabi, S., Uzan, B., Naguibneva, I., Rucci, J., Fahy, L., Calvo, J., Arcangeli, M.L., Mazurier, F., Pflumio, F., and Haddad, R. (2019). Hypoxia Regulates Lymphoid Development of Human Hematopoietic Progenitors. *Cell Rep* 29, 2307-2320 e2306.
- Chang, R.B., Strohlic, D.E., Williams, E.K., Umans, B.D., and Liberles, S.D. (2015). Vagal Sensory Neuron Subtypes that Differentially Control Breathing. *Cell* 161, 622-633.
- Cieslar-Pobuda, A., Knoflach, V., Ringh, M.V., Stark, J., Likus, W., Siemianowicz, K., Ghavami, S., Hudecki, A., Green, J.L., and Los, M.J. (2017). Transdifferentiation and reprogramming: Overview of the processes, their similarities and differences. *Biochim Biophys Acta Mol Cell Res* 1864, 1359-1369.
- Cirovic, B., Schonheit, J., Kowenz-Leutz, E., Ivanovska, J., Klement, C., Pronina, N., Begay, V., and Leutz, A. (2017). C/EBP-Induced Transdifferentiation Reveals Granulocyte-Macrophage Precursor-like Plasticity of B Cells. *Stem Cell Reports* 8, 346-359.
- Collombet, S., van Oevelen, C., Sardina Ortega, J.L., Abou-Jaoude, W., Di Stefano, B., Thomas-Chollier, M., Graf, T., and Thieffry, D. (2017). Logical modeling of lymphoid and myeloid cell specification and transdifferentiation. *Proc Natl Acad Sci U S A* 114, 5792-5799.
- Corcoran, S., and Brückner, K. (2020). Quantification of blood cells in *Drosophila* and other insects. *Springer Protocols Handbooks: Immunity in Insects Sandrelli F, Tettamanti G, editors*, 65-77.
- Cutz, E., Yeger, H., and Pan, J. (2007). Pulmonary neuroendocrine cell system in pediatric lung disease-recent advances. *Pediatr Dev Pathol* 10, 419-435.
- Davies, L.C., Jenkins, S.J., Allen, J.E., and Taylor, P.R. (2013). Tissue-resident macrophages. *Nat Immunol* 14, 986-995.
- Di Tullio, A., Vu Manh, T.P., Schubert, A., Castellano, G., Mansson, R., and Graf, T. (2011). CCAAT/enhancer binding protein alpha (C/EBP(alpha))-induced transdifferentiation of pre-B cells into macrophages involves no overt retrodifferentiation. *Proc Natl Acad Sci U S A* 108, 17016-17021.

- Dudzic, J.P., Kondo, S., Ueda, R., Bergman, C.M., and Lemaitre, B. (2015). *Drosophila* innate immunity: regional and functional specialization of prophenoloxidases. *BMC Biol* 13, 81.
- Duvic, B., Hoffmann, J.A., Meister, M., and Royet, J. (2002). Notch signaling controls lineage specification during *Drosophila* larval hematopoiesis. *Curr Biol* 12, 1923-1927.
- Gold, K.S., and Brückner, K. (2014). *Drosophila* as a model for the two myeloid blood cell systems in vertebrates. *Exp Hematol* 42, 717-727.
- Gold, K.S., and Brückner, K. (2015). Macrophages and cellular immunity in *Drosophila melanogaster*. *Semin Immunol* 27, 357-368.
- Gorr, T.A., Gassmann, M., and Wappner, P. (2006). Sensing and responding to hypoxia via HIF in model invertebrates. *J Insect Physiol* 52, 349-364.
- Haase, V.H. (2013). Regulation of erythropoiesis by hypoxia-inducible factors. *Blood Rev* 27, 41-53.
- Hamada, F.N., Rosenzweig, M., Kang, K., Pulver, S.R., Ghezzi, A., Jegla, T.J., and Garrity, P.A. (2008). An internal thermal sensor controlling temperature preference in *Drosophila*. *Nature* 454, 217-220.
- Hanoun, M., Maryanovich, M., Arnal-Estape, A., and Frenette, P.S. (2015). Neural regulation of hematopoiesis, inflammation, and cancer. *Neuron* 86, 360-373.
- Hayashi, S., and Kondo, T. (2018). Development and Function of the *Drosophila* Tracheal System. *Genetics* 209, 367-380.
- Holz, A., Bossinger, B., Strasser, T., Janning, W., and Klapper, R. (2003). The two origins of hemocytes in *Drosophila*. *Development* 130, 4955-4962.
- Imanirad, P., and Dzierzak, E. (2013). Hypoxia and HIFs in regulating the development of the hematopoietic system. *Blood Cells Mol Dis* 51, 256-263.
- Inokuchi, K., Kato, A., Hiraia, K., Hishinuma, F., Inoue, M., and Ozawa, F. (1996). Increase in activin beta A mRNA in rat hippocampus during long-term potentiation. *FEBS Lett* 382, 48-52.
- Kaupp, U.B., and Seifert, R. (2002). Cyclic nucleotide-gated ion channels. *Physiol Rev* 82, 769-824.
- Krzemien, J., Dubois, L., Makki, R., Meister, M., Vincent, A., and Crozatier, M. (2007). Control of blood cell homeostasis in *Drosophila* larvae by the posterior signalling centre. *Nature* 446, 325-328.
- Kuhn, D.T., Sawyer, M., Packert, G., Turenchalk, G., Mack, J.A., Sprey, T.E., Gustavson, E., and Kornberg, T.B. (1992). Development of the *D. melanogaster* caudal segments involves suppression of the ventral regions of A8, A9 and A10. *Development* 116, 11-20.
- Kumar, A., and Brockes, J.P. (2012). Nerve dependence in tissue, organ, and appendage regeneration. *Trends in neurosciences* 35, 691-699.
- Lanot, R., Zachary, D., Holder, F., and Meister, M. (2001). Postembryonic hematopoiesis in *Drosophila*. *Dev Biol* 230, 243-257.
- Lebestky, T., Chang, T., Hartenstein, V., and Banerjee, U. (2000). Specification of *Drosophila* hematopoietic lineage by conserved transcription factors. *Science* 288, 146-149.
- Lebestky, T., Jung, S.H., and Banerjee, U. (2003). A Serrate-expressing signaling center controls *Drosophila* hematopoiesis. *Genes Dev* 17, 348-353.

Lefrancais, E., Ortiz-Munoz, G., Caudrillier, A., Mallavia, B., Liu, F., Sayah, D.M., Thornton, E.E., Headley, M.B., David, T., Coughlin, S.R., *et al.* (2017). The lung is a site of platelet biogenesis and a reservoir for haematopoietic progenitors. *Nature* 544, 105-109.

Leitao, A.B., and Sucena, E. (2015). *Drosophila* sessile hemocyte clusters are true hematopoietic tissues that regulate larval blood cell differentiation. *Elife* 4.

Li, P., Burke, S., Wang, J., Chen, X., Ortiz, M., Lee, S.C., Lu, D., Campos, L., Goulding, D., Ng, B.L., *et al.* (2010). Reprogramming of T cells to natural killer-like cells upon Bcl11b deletion. *Science* 329, 85-89.

Lu, A., Zhang, Q., Zhang, J., Yang, B., Wu, K., Xie, W., Luan, Y.X., and Ling, E. (2014). Insect prophenoloxidase: the view beyond immunity. *Front Physiol* 5, 252.

Majmundar, A.J., Wong, W.J., and Simon, M.C. (2010). Hypoxia-inducible factors and the response to hypoxic stress. *Mol Cell* 40, 294-309.

Makhijani, K., Alexander, B., Rao, D., Petraki, S., Herboso, L., Kukar, K., Batool, I., Wachner, S., Gold, K.S., Wong, C., *et al.* (2017). Regulation of *Drosophila* hematopoietic sites by Activin-beta from active sensory neurons. *Nat Commun* 8, 15990.

Makhijani, K., Alexander, B., Tanaka, T., Rulifson, E., and Brückner, K. (2011). The peripheral nervous system supports blood cell homing and survival in the *Drosophila* larva. *Development* 138, 5379-5391.

Makhijani, K., and Brückner, K. (2012). Of blood cells and the nervous system: Hematopoiesis in the *Drosophila* larva. *Fly (Austin)* 6, 254-260.

Markus, R., Laurinyecz, B., Kurucz, E., Honti, V., Bajusz, I., Sipos, B., Somogyi, K., Kronhamn, J., Hultmark, D., and Ando, I. (2009). Sessile hemocytes as a hematopoietic compartment in *Drosophila melanogaster*. *Proc Natl Acad Sci U S A* 106, 4805-4809.

Martin, J.F., Slater, D.N., and Trowbridge, E.A. (1983). Abnormal intrapulmonary platelet production: a possible cause of vascular and lung disease. *Lancet* 1, 793-796.

Mazzone, S.B., and Undem, B.J. (2016). Vagal Afferent Innervation of the Airways in Health and Disease. *Physiol Rev* 96, 975-1024.

McGuire, S.E., Le, P.T., Osborn, A.J., Matsumoto, K., and Davis, R.L. (2003). Spatiotemporal rescue of memory dysfunction in *Drosophila*. *Science* 302, 1765-1768.

Miyashita, T., Oda, Y., Horiuchi, J., Yin, J.C., Morimoto, T., and Saitoe, M. (2012). Mg(2+) block of *Drosophila* NMDA receptors is required for long-term memory formation and CREB-dependent gene expression. *Neuron* 74, 887-898.

Morton, D.B. (2004). Atypical soluble guanylyl cyclases in *Drosophila* can function as molecular oxygen sensors. *J Biol Chem* 279, 50651-50653.

Morton, D.B. (2011). Behavioral responses to hypoxia and hyperoxia in *Drosophila* larvae: molecular and neuronal sensors. *Fly (Austin)* 5, 119-125.

Morton, D.B., Langlais, K.K., Stewart, J.A., and Vermehren, A. (2005). Comparison of the properties of the five soluble guanylyl cyclase subunits in *Drosophila melanogaster*. *J Insect Sci* 5, 12.

Morton, D.B., Stewart, J.A., Langlais, K.K., Clemens-Grisham, R.A., and Vermehren, A. (2008). Synaptic transmission in neurons that express the *Drosophila* atypical soluble guanylyl cyclases,

Gyc-89Da and Gyc-89Db, is necessary for the successful completion of larval and adult ecdysis. *J Exp Biol* 211, 1645-1656.

Mukherjee, T., Kim, W.S., Mandal, L., and Banerjee, U. (2011). Interaction between Notch and Hif- α in development and survival of *Drosophila* blood cells. *Science* 332, 1210-1213.

Pavlov, V.A., and Tracey, K.J. (2012). The vagus nerve and the inflammatory reflex--linking immunity and metabolism. *Nature reviews Endocrinology* 8, 743-754.

Perdiguerro, E.G., and Geissmann, F. (2016). The development and maintenance of resident macrophages. *Nat Immunol* 17, 2-8.

Pesaresi, M., Sebastian-Perez, R., and Cosma, M.P. (2019). Dedifferentiation, transdifferentiation and cell fusion: in vivo reprogramming strategies for regenerative medicine. *Febs J* 286, 1074-1093.

Petraki, S., Alexander, B., and Brückner, K. (2015). Assaying Blood Cell Populations of the *Drosophila melanogaster* Larva. *J Vis Exp*.

Pifferi, S., Boccaccio, A., and Menini, A. (2006). Cyclic nucleotide-gated ion channels in sensory transduction. *FEBS Lett* 580, 2853-2859.

Pokorski, M., Takeda, K., and Okada, Y. (2016). Oxygen Sensing Mechanisms: A Physiological Penumbra. *Adv Exp Med Biol* 952, 1-8.

Rapino, F., Robles, E.F., Richter-Larrea, J.A., Kallin, E.M., Martinez-Climent, J.A., and Graf, T. (2013). C/EBP α induces highly efficient macrophage transdifferentiation of B lymphoma and leukemia cell lines and impairs their tumorigenicity. *Cell Rep* 3, 1153-1163.

Reid, A., and Tursun, B. (2018). Transdifferentiation: do transition states lie on the path of development? *Curr Opin Syst Biol* 11, 18-23.

Rizki, M.T., and Rizki, R.M. (1959). Functional significance of the crystal cells in the larva of *Drosophila melanogaster*. *J Biophys Biochem Cytol* 5, 235-240.

Schindelin, J., Arganda-Carreras, I., Frise, E., Kaynig, V., Longair, M., Pietzsch, T., Preibisch, S., Rueden, C., Saalfeld, S., Schmid, B., *et al.* (2012). Fiji: an open-source platform for biological-image analysis. *Nat Methods* 9, 676-682.

Sieweke, M.H., and Allen, J.E. (2013). Beyond stem cells: self-renewal of differentiated macrophages. *Science* 342, 1242974.

Sinenko, S.A., and Mathey-Prevot, B. (2004). Increased expression of *Drosophila* tetraspanin, Tsp68C, suppresses the abnormal proliferation of ytr-deficient and Ras/Raf-activated hemocytes. *Oncogene* 23, 9120-9128.

Siripin, D., Kheolamai, P., Y, U.P., Supokawej, A., Wattanapanitch, M., Klincumhom, N., Laowtammathron, C., and Issaragrisil, S. (2015). Transdifferentiation of erythroblasts to megakaryocytes using FLI1 and ERG transcription factors. *Thromb Haemost* 114, 593-602.

Song, W., Onishi, M., Jan, L.Y., and Jan, Y.N. (2007). Peripheral multidendritic sensory neurons are necessary for rhythmic locomotion behavior in *Drosophila* larvae. *Proc Natl Acad Sci U S A* 104, 5199-5204.

Stewart, S., Koh, T.W., Ghosh, A.C., and Carlson, J.R. (2015). Candidate ionotropic taste receptors in the *Drosophila* larva. *Proc Natl Acad Sci U S A* 112, 4195-4201.

Tattikota, S.G., Hu, Y., Liu, Y., Cho, B., Barrera, V., Steinbaugh, M., Yoon, S.-H., Comjean, A., Li, F., Dervis, F., *et al.* (2019). A single-cell survey of *Drosophila* blood. *bioRxiv*, 2019.2012.2020.884999.

Tokusumi, T., Shoue, D.A., Tokusumi, Y., Stoller, J.R., and Schulz, R.A. (2009). New hemocyte-specific enhancer-reporter transgenes for the analysis of hematopoiesis in *Drosophila*. *Genesis* 47, 771-774.

Vermehren, A., Langlais, K.K., and Morton, D.B. (2006). Oxygen-sensitive guanylyl cyclases in insects and their potential roles in oxygen detection and in feeding behaviors. *J Insect Physiol* 52, 340-348.

Vermehren-Schmaedick, A., Ainsley, J.A., Johnson, W.A., Davies, S.A., and Morton, D.B. (2010). Behavioral responses to hypoxia in *Drosophila* larvae are mediated by atypical soluble guanylyl cyclases. *Genetics* 186, 183-196.

Vermehren-Schmaedick, A., Scudder, C., Timmermans, W., and Morton, D.B. (2011). *Drosophila* gustatory preference behaviors require the atypical soluble guanylyl cyclases. *J Comp Physiol A Neuroethol Sens Neural Behav Physiol* 197, 717-727.

Vlisidou, I., and Wood, W. (2015). *Drosophila* blood cells and their role in immune responses. *Febs J* 282, 1368-1382.

Wu, Q., Wen, T., Lee, G., Park, J.H., Cai, H.N., and Shen, P. (2003). Developmental control of foraging and social behavior by the *Drosophila* neuropeptide Y-like system. *Neuron* 39, 147-161.

Xiang, Y., Yuan, Q., Vogt, N., Looger, L.L., Jan, L.Y., and Jan, Y.N. (2010). Light-avoidance-mediating photoreceptors tile the *Drosophila* larval body wall. *Nature* 468, 921-926.

Xie, H., Ye, M., Feng, R., and Graf, T. (2004). Stepwise reprogramming of B cells into macrophages. *Cell* 117, 663-676.

Yang, H., Kronhamn, J., Ekstrom, J.O., Korkut, G.G., and Hultmark, D. (2015). JAK/STAT signaling in *Drosophila* muscles controls the cellular immune response against parasitoid infection. *EMBO Rep* 16, 1664-1672.

Figure Legends

Figure 1. Crystal cells in the *Drosophila* larva are generated by transdifferentiation

(A) Development of crystal cell numbers over time. Crystal cells per larva, assessed by melanization, relative to larval size and developmental stage. Genotype is *w¹¹¹⁸*, n=155. Mean and standard deviation, regression analysis.

(B) Development of total hemocyte numbers over time. Total hemocytes per larva, genotype is *HmlΔGAL4, UAS-GFP; He-GAL4*; n=107. Mean and standard deviation, regression analysis.

(C-C'') Localization of plasmatocytes and crystal cells in the 3rd instar larva,; genotype is *BcF2-GFP/HmlΔ-DsRed*; plasmatocytes labeled by *HmlΔ-DsRed* (red); crystal cells labeled by *BcF2-GFP* (green); lateral view, posterior right.

(D-D') Model of distribution of plasmatocyte (red) and crystal cells (orange) in *Drosophila* larva, relevant sensory neuron clusters of the hematopoietic pockets (green); lateral view, posterior right.

(E-E'') Scheme of phagocytosis lineage tracing assay. Blue fluorescent latex beads are injected into early 3rd instar larvae, cells are released after indicated incubation times; fraction of cells containing phagocytosed beads are determined. Possible outcomes are depicted with crystal cells in orange, plasmatocytes in red, progenitors in grey.

(F) Sample image of analyzed cells; genotype *BcF2-GFP/HmlΔ-DsRed*; crystal cells in green, plasmatocytes in red; blue arrowheads indicate crystal cells with incorporated blue beads.

(G) Quantification of samples as in (G); fraction of plasmatocytes and crystal cells containing blue beads at time 1h, 4, 22h after injection; n=21; mean and standard deviation.

Figure 2. Sensory Neuron activity regulates transdifferentiation to crystal cells

(A) Plasmatocytes colocalize with sensory neurons in all hematopoietic pockets; genotype *21-7-GAL4, UAS-CD8-GFP, HmlΔDsRed/CyO*; lateral view, posterior right.

(B) Crystal cells also colocalize with sensory neurons but are mainly found in a cluster at the caudal end of the larva; genotype *21-7-GAL4, UAS-CD8-GFP/+; BCF6-mCherry/+*; lateral view, posterior right.

(C) Treatment of larvae with the AchR agonist carbachol to mimic sensory neuron activation, treatment for 4h; genotype is *yw*; quantification of crystal cells by melanization; control n=65 (+45); carbachol n=34 (+50). Individual value plot with mean and standard deviation, two-way ANOVA.

(D) Transient silencing of sensory neurons, quantification of crystal cells by melanization; genotypes are experiment *21-7-GAL4, UAS-CD8GFP, HmlΔ-DsRed/ UAS-Kir2.1; tubGAL80ts/ +* and control *21-7-GAL4, UAS-CD8GFP, HmlΔ-DsRed/ +; tubGAL80ts/ +*. Larvae induced at 29°C for 22h. Mean and standard deviation, two-way ANOVA.

(E, F) Phagocytosis lineage tracing, genotypes are experiment *21-7-GAL4, UAS-CD8GFP, HmlΔ-DsRed/ UAS-Kir2.1; BcF6-GFP/ tubGAL80ts*, and control *21-7-GAL4, UAS-CD8GFP, HmlΔ-DsRed/ +; BcF6-GFP/ tubGAL80ts*.

(E) Sample image of analyzed cells, plasmatocytes (red), crystal cells (green), injected beads (blue).

(F) Quantification of samples as in (E); fraction of plasmatocytes and crystal cells containing blue beads, experiment n=12 and control n=12. Mean and standard deviation, two-way ANOVA.

Figure 3. Crystal cells are clustered around the sensory cones and are promoted by sensory cone neurons

(A-D) Localization of sensory neurons, plasmatocytes and crystal cells, caudal view of larvae; scale bars 0.25mm.

(A) Sensory neurons (green), genotype *21-7-GAL4, UAS-CD8-GFP, HmlΔ-DsRed/CyO*; 3rd instar larva.

(B) Plasmatocytes (green) and crystal cells (red), genotype *HmlΔ-GAL4, UAS-GFP; BcF6-mCherry*; 2nd instar larva.

(C) Crystal cells (red) and sensory neurons (green), genotype *21-7-GAL4, UAS-CD8-GFP/+; BcF6-mCherry/+*; 2nd instar larva.

(D) Crystal cells (red) and sensory neurons (green), *21-7-GAL4, UAS-CD8-GFP/+; BcF6-mCherry/+*; 3rd instar larva.

(A'-D') Models corresponding to (A-D), respectively, plasmatocytes red, crystal cells orange, sensory neurons green; caudal view.

(A''-D'') Models, lateral view, corresponding to (A-C and A'-C'), respectively; lateral view.

(E) *Gyc89Db-GAL4* driver expressing GFP in sensory cone neurons (green), lateral view, genotype is *UAS-GFP/+; Gyc89Db-GAL4/+*; lateral view, posterior right; scale bar 0.5mm.

(F) Larva as in (E), caudal view.

(G) Ablation of sensory cone neurons affects crystal cells; quantification of crystal cells per larva by melanization. Genotypes are experiment *UAS-Hid ala5/+; Gyc89Db-GAL4/tubGAL80ts*, n=34 and control *Gyc89Db-GAL4/tubGAL80ts*, n=34. Crosses were raised at 18°C and temperature shifted to 29 °C for 16 h. Individual value plot with mean and standard deviation, two-way ANOVA.

(H) Transient activation of TrpA1 in sensory cone neurons; quantification of crystal cells per larva by melanization. Genotypes are experiment *UAS-TrpA1/+; Gyc89Db-GAL4, / +*, n=46, and control *Gyc89Db-GAL4/+*, n=48; in addition, one experiment F1 cohort *UAS-TrpA1/+; Gyc89Db-GAL4, / +*, n=47, was maintained as uninduced control at RT. Crosses were raised at RT and temperature shifted to 29°C for 4 hours;. Individual value plot with mean and standard deviation, two-way ANOVA.

Figure 4. Oxygen sensing through Gycs in sensory cone neurons drives plasmatocyte-to-crystal cell transdifferentiation

(A) RNAi silencing of *Gyc88E* in sensory cone neurons results in reduced crystal cell numbers determined by melanization; genotypes are experiment *Gyc89Db-GAL4/UAS-Gyc88ERNAi*, n=45 and control *Gyc89Db-GAL4/+*, n=45. Individual value plot with mean and standard deviation, two-way ANOVA.

(B) Phagocytosis lineage tracing, effect of *Gyc88E* RNAi in sensory cone neurons on transdifferentiation; genotypes are experiment *21-7-GAL4, UA5-CD8-GFP, HmlΔ-DsRed/+; BcF6-GFP/ UAS-Gyc88ERNAi*, n=11 and control *21-7-GAL4, UA5-CD8-GFP, HmlΔ-DsRed/+; BcF6-GFP/+*, n=16. Bar chart with mean and standard deviation, two-way ANOVA.

(C) Effect of hypoxia (5% O₂) on crystal cell number per larva determined by melanization; genotype is *w¹¹¹⁸*; hypoxia n=46 and normoxia n=48. Individual value plot with mean and standard deviation, two-way ANOVA.

(D) Phagocytosis lineage tracing, effect of hypoxia (5% O₂) on transdifferentiation; genotype is *HmlΔ-GAL4, UAS-GFP; BcF6-mCherry*; hypoxia n=14 and normoxia n=15. Bar chart with mean and standard deviation, two-way ANOVA.

(E) Model. Sensory cone neurons detect oxygen by cytoplasmic Gyc heterodimeric oxygen sensors. Gycs convert GTP to cGMP, which activates CNG channels, resulting in influx of calcium (Ca²⁺) leading to downstream signaling and neuronal activation. Active neurons induce plasmatocyte-to-crystal cell transdifferentiation.

Supplemental Materials

Supplemental Figure 1. Methods of crystal cell labeling

(A) Heat induced melanization of crystal cells. Genotype is *lz-GAL4;UAS-GFP*

(B) Fluorescent reporter labeling to visualize, and quantify, crystal cells. Genotype is *lz-GAL4;UAS-GFP*. Note that the labeled crystal cell pattern by both methods is very similar.

Supplemental Figure 2. Limited transient sensory neuron silencing does not affect total hemocyte numbers

(A) Transient silencing of sensory neurons, quantification of total hemocytes; genotypes are *21-7-GAL4, UAS-CD8-GFP, HmlΔ-DsRed/ UAS-Kir2.1; tubGAL80ts/+*, n=12 and control *21-7-GAL4, UAS-CD8-GFP, HmlΔ-DsRed/+; tubGAL80ts/+*, n=13. Larvae induced at 29°C for 22h. Mean and standard deviation, two-way ANOVA

Supplemental Figure 3. Hypoxia affects crystal cell counts but not total hemocyte numbers

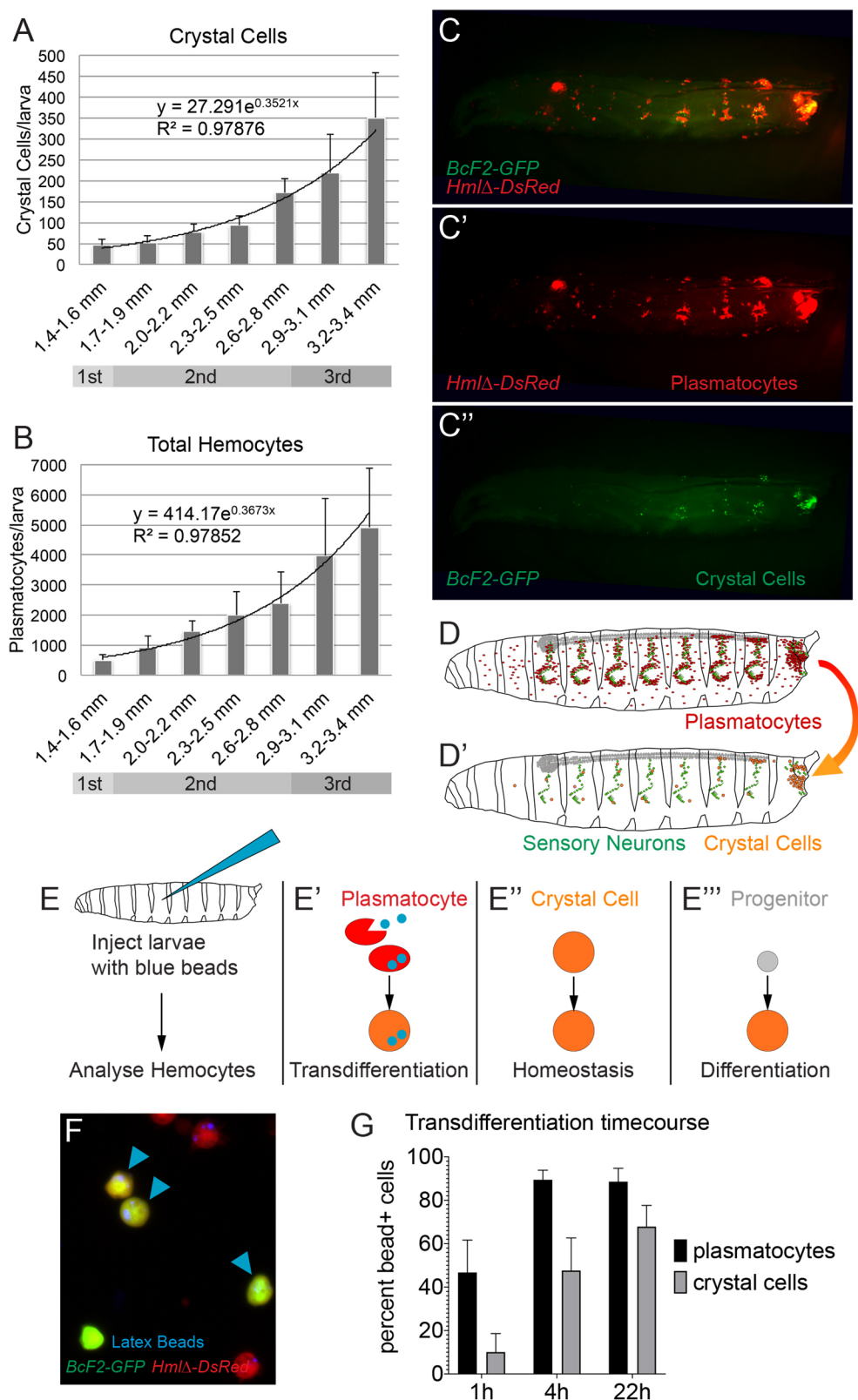
(A) Effect of 8% hypoxia on crystal cell number determined by melanization; genotype is *w1118*; hypoxia n=19 and normoxia control n=18. Individual value plot with mean and standard deviation, two-way ANOVA.

(B) Total hemocyte number under conditions of hypoxia (5% O₂) and normoxia; genotype is *HmlΔ-GAL4, UAS-GFP; BcF6-mCherry*; hypoxia n=14 and normoxia control n=14. Mean and standard deviation, two-way ANOVA.

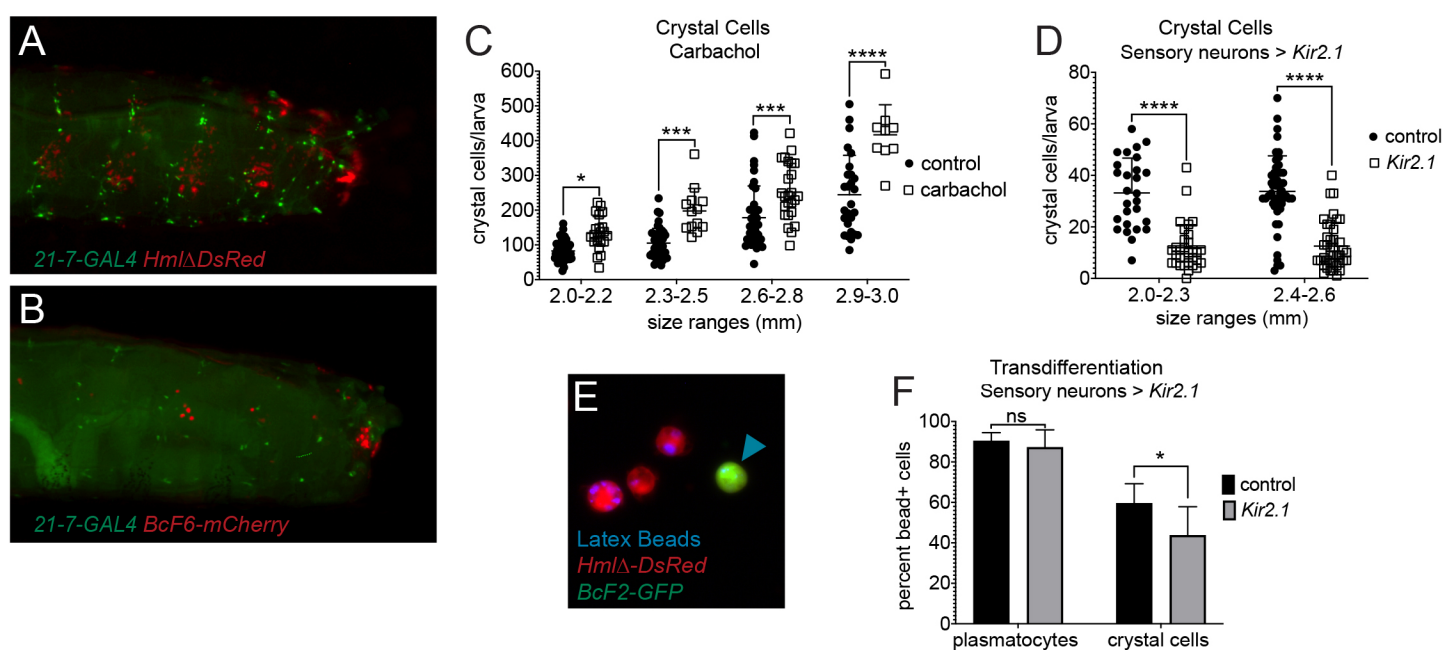
Supplemental Figure 4. Models

(A) Stimulated by oxygen, activated sensory cone neurons produce signal/s that drive transdifferentiation of a fraction of plasmatocytes to crystal cells. According to this model, transdifferentiation is triggered by contacting the sensory neuron signal, therefore plasmatocytes in anatomical proximity to the sensory cone neurons are most likely to convert into crystal cells.

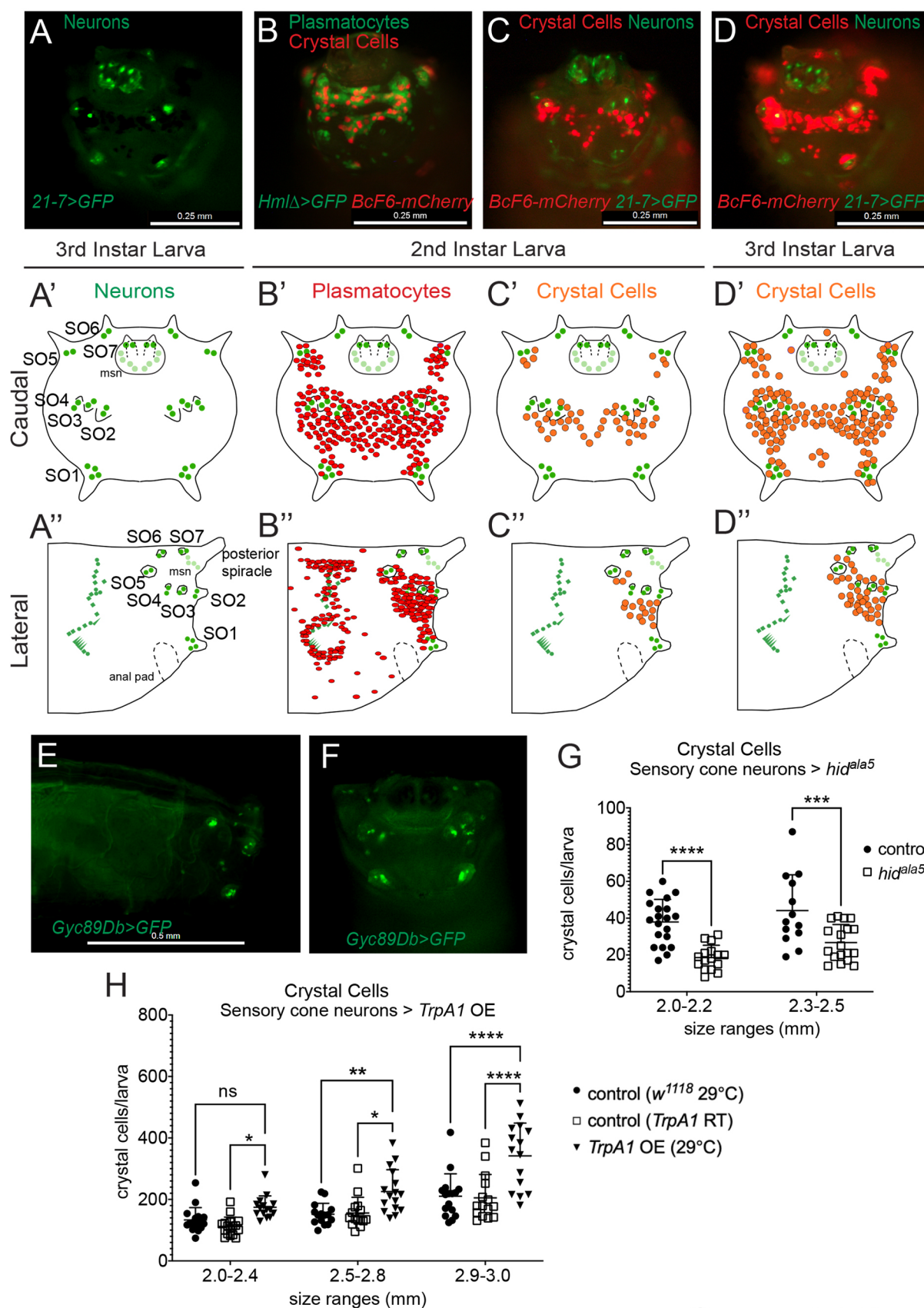
(B) Model illustrating exposure of the caudal end of *Drosophila* larvae including the sensory cones and posterior spiracles to the air, while burying in food. Mature larvae leave the food in preparation of pupariation, now fully exposed to the air.



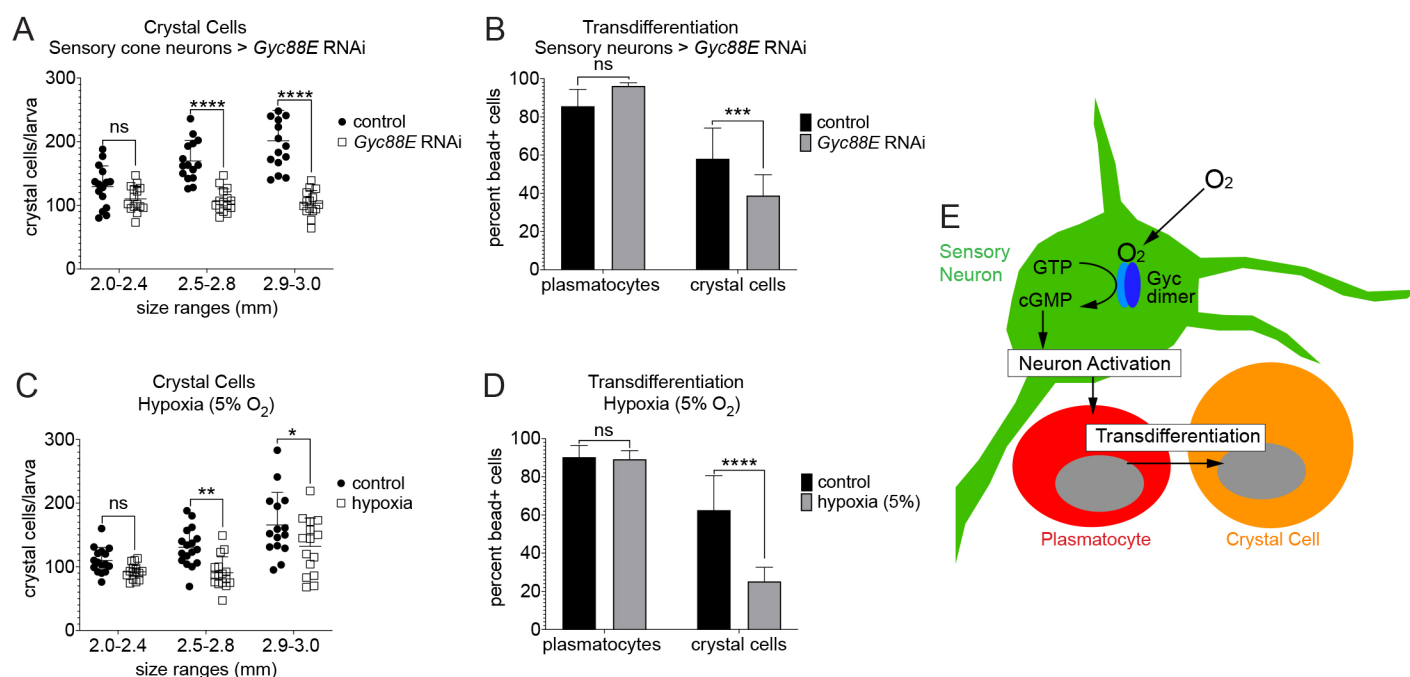
Corcoran et al., Figure 1



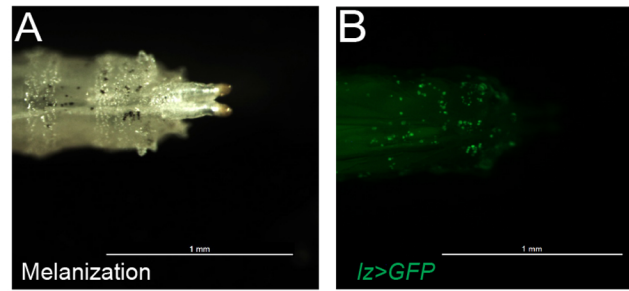
Corcoran et al. Figure 2



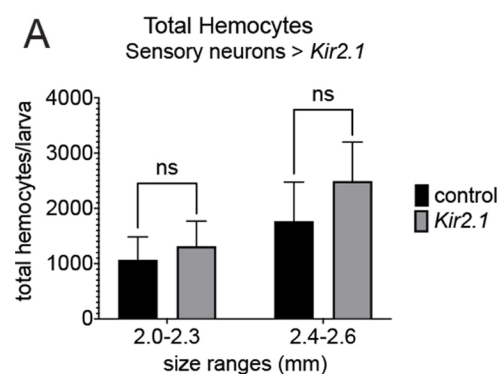
Corcoran et al. Figure 3



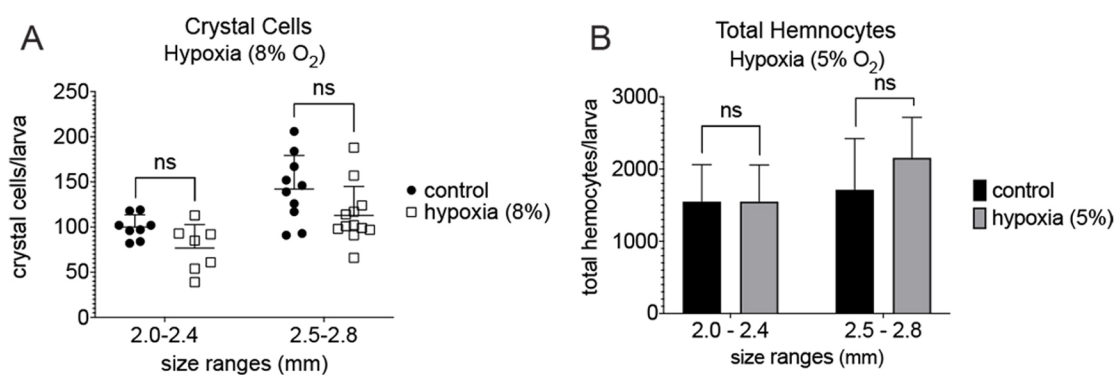
Corcoran et al. Figure 4



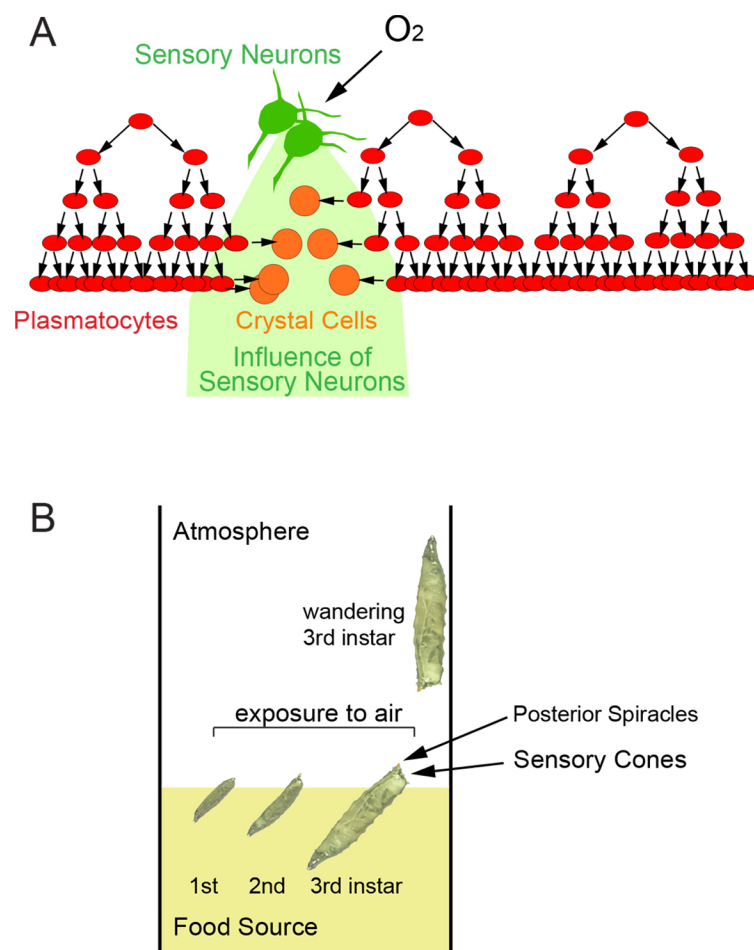
Corcoran et al. Supplemental Figure 1



Corcoran et al. Supplemental Figure 2



Corcoran et al. Supplemental Figure 3



Corcoran et al. Supplemental Figure 4